
Time Delay Estimation of Traffic Congestion Propagation based on Transfer Entropy

YongKyung Oh¹, JiIn Kwak², JuYeong Lee¹, Sungil Kim^{1,2}

¹Department of Industrial Engineering, ²Artificial Intelligence Graduate School
Ulsan National Institute of Science and Technology (UNIST)
`{ok19925, jiin1938, passionlee428, sungil.kim}@unist.ac.kr`

Abstract

Considering how congestion will propagate in the near future, understanding traffic congestion propagation has become crucial in GPS navigation systems for providing users with a more accurate estimated time of arrival (ETA). However, providing the exact ETA during congestion is a challenge owing to the complex propagation process between roads and high uncertainty regarding the future behavior of the process. Recent studies have focused on finding frequent congestion propagation patterns and determining the propagation probabilities. By contrast, this study proposes a novel time delay estimation method for traffic congestion propagation between roads using lag-specific transfer entropy (TE). Nonlinear normalization with a sliding window is used to effectively reveal the causal relationship between the source and target time series in calculating the TE. Moreover, Markov bootstrap techniques were adopted to quantify the uncertainty in the time delay estimator. To the best of our knowledge, the time delay estimation method presented in this article is the first to determine the time delay between roads for any congestion propagation pattern. The proposed method was validated using simulated data as well as real user trajectory data obtained from a major GPS navigation system applied in South Korea.

1 Introduction

Traffic congestion has been a universal problem for urban cities owing to the dramatic growth of population and the corresponding increase in vehicles, the economy, infrastructure, and proliferation of delivery services, among other factors. Congestion can cause severe operational problems, including traffic delays, and a waste of time and energy [11]. Moreover, traffic congestion affects nearby roads and causes additional congestion, particularly in all traffic leading to congested roads [15], causing greater damage to the traffic network. This phenomenon is called congestion propagation and is a chronic problem for most urban cities with large traffic networks.

In particular, understanding traffic congestion propagation has become crucial in GPS navigation systems to provide users with a more accurate estimated time of arrival (ETA), considering how congestion propagation patterns in the near future. However, it is challenging to provide an exact ETA under cases of congestion owing to the complex propagation process between roads and high uncertainty about the future behavior of the process. Figure 1 illustrates the motivation for this study. Without understanding traffic congestion propagation, the GPS navigation system suggests the optimal route based on the road conditions when the driver requests an ETA, as shown in Figure 1(a). The blue lines in the figure represent the suggested optimal routes. However, the optimal route in Figure 1(a) faces severe traffic congestion when the driver arrives in a congested area because congestion propagates while the driver is moving. If the GPS navigation system can identify the time delays between roads owing to congestion propagation, different optimal routes should be suggested,

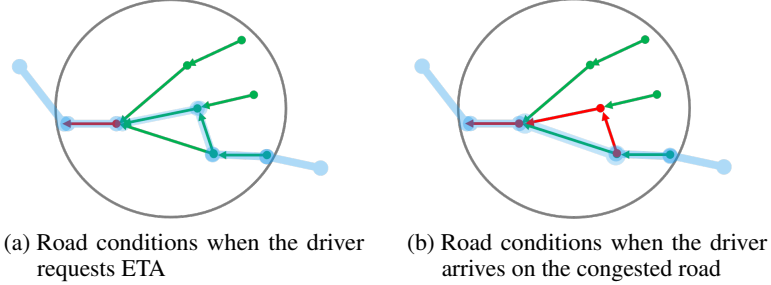


Figure 1: Motivating example: GPS navigation system recommending a travel route (blue lines) based on the related road conditions (red segment, congested; green segment, free flow).

as shown in Figure 1(b). Hence, to provide an accurate ETA in urban cities, a time delay estimation of traffic congestion propagation is inevitable.

In this paper, we propose a new time delay estimation method for traffic congestion propagation between roads using lag-specific Transfer Entropy (TE). Our main contributions are as follows:

- We provide a model-free approach to estimate congestion propagation delays using a lag-specific TE estimator in complex urban road systems.
- We show that a nonlinear normalization with a sliding window, as a time series preprocessing method, is more effective than existing approaches in revealing the causal relationship between traffic speed data.
- We assess the accuracy of the time delay estimate using Markov bootstrap techniques.
- We validate the proposed method through numerical simulations as well as real user trajectory data obtained from one of the major GPS navigation systems in South Korea.

This paper is organized as follows: Section 2 reviews related studies. Section 3 introduces the bootstrap for Markov chains and a lag-specific transfer entropy with bias correction, and Section 4 proposes our new time delay estimation method. Section 5 and 6 validate the proposed method using simulated data and real congestion propagation data in a road network, respectively. Finally, Section 7 provides some concluding remarks regarding this study.

2 Related Work

2.1 Congestion Propagation Pattern Analysis

Recent studies on congestion propagation patterns have been widely conducted, focusing on an analysis of spatio-temporal patterns. The prediction of propagation patterns can be divided into statistical methods and deep learning (DL) based approaches. Statistical methods focus mainly on finding the most frequent propagation footprints from the past, which have occurred owing to recurring congestion. The STOTree and frequent subtree algorithms were proposed based on outlier detection approaches for each road segment [12]. Propagation Graphs (Pro-Graphs) were used to predict patterns of congestion propagation [26]. Meanwhile, DL-based methods consider spatio-temporal correlations during the process of predicting the congestion propagation. LSTM-based methods are used to predict the propagation patterns in the next time steps based on historical data [2, 5]. [28] defined the congestion intensity level and predicted the future congestion level by applying auto-encoder to generated traffic network images. However, most recent works have focused on detecting frequent congestion propagation patterns and calculating propagation probabilities. To the best of our knowledge, there is no time delay estimation method for traffic congestion propagation using GPS trajectory data.

2.2 Information Transfer Delays

To discover the relationships between neighboring road segments, several methods have been used to analyze interactions among multiple time series, ranging from model-based approaches operating in the time or frequency domains to model-free approaches operating in the information domain [17].

Model-based approaches are useful under certain assumptions; however, such simplified assumptions may not be valid in practice. For this reason, model-free techniques have been widely applied in complex systems [6].

Information theory provides a natural framework for a model-free analysis of coupled systems. As a model-free approach, transfer entropy (TE) [18] has been a popular measure of the directional interaction between two time series, because of its inherent ability to incorporate directional and dynamical information, its sensitivity to both linear and nonlinear interactions, and its close connection with Granger causality [7, 1]. In principle, TE does not assume any particular model for the interaction in coupled systems. Thus, the sensitivity of TE to all order correlations is an advantage for an exploratory analysis of Granger causality or other model-based approaches [22]. Owing to the several advantages of transfer entropy described above, it has been applied to various domains that use time-series data such as biomedical data [6, 10, 22], stock prices in the financial field [19, 27, 21], and chemical analysis [9, 13].

Time delays naturally arise as a consequence of propagation effects in coupled systems. Thus, it is of great importance to evaluate the exact coupling delays among interacting time series for uncovering dynamic information in complex networks [24]. To quantify the information transfer between time series in complex networks and to detect the timing when such a transfer occurs, several lag-specific TE estimators have been proposed [6, 24]. [25] used transfer entropy to discover the real dynamic process of flight-delay propagation among multiple airports. However, to the best of our knowledge, our proposed method is the first to use lag-specific TE to predict the time delay for congestion propagation in road traffic networks.

3 Background

3.1 Bootstrap for Markov Chains

Suppose that $\{X_t\}_{t \geq 1}$ be a stationary Markov chain with a finite state space $S = \{s_1, \dots, s_n\}$, where $n \in \mathbb{N}$. Let $\mathbf{P} = (p_{ij}) \in \mathbb{R}^{n \times n}$ be a transition probability matrix of the chain and the stationary distribution by $\boldsymbol{\pi} = (\pi_1, \dots, \pi_n)$. Thus, for any $1 \leq i, j \leq n$, $p_{ij} = P(X_{t+1} = s_j | X_t = s_i)$ and $\pi_i = P(X_t = s_i)$. Given a time series $\{X_1, \dots, X_L\}$ of size L from a stationary Markov chain, we can estimate π_i and p_{ij} as

$$\hat{\pi}_i = \frac{1}{L} \sum_{t=1}^L \mathbb{1}(X_t = s_i), \quad \hat{p}_{ij} = \frac{1}{\hat{\pi}_i L} \sum_{t=1}^L \mathbb{1}(X_t = s_i, X_{t+1} = s_j). \quad (1)$$

The bootstrap observations $\{X_1^*, \dots, X_L^*\}$ can now be generated using the estimated transition matrix and the marginal distribution in Eq.(1) [8].

- 1) Generate a random variable X_1^* from the discrete distribution on $\{1, \dots, n\}$ that assigns mass $\hat{\pi}_i$ to s_i , $1 \leq i \leq n$.
- 2) Generate a random variable X_{t+1}^* from the discrete distribution on $\{1, \dots, n\}$ that assigns mass \hat{p}_{ij} to j , $1 \leq j \leq n$, where s_i is the value of X_t^* .
- 3) Repeat step 2) until a simulated time series $\{X_1^*, \dots, X_L^*\}$ has been obtained.

3.2 Lag-specific Transfer Entropy

TE is a measurement of directed information flow [18] based on the concept of Shannon entropy [20] in the area of information theory. For a discrete random variable I with probability distribution $p(i)$, Shannon entropy represents the average number of bits required to optimally encode independent draws, which can be calculated as follows:

$$H(I) = - \sum_i p(i) \log_2 p(i). \quad (2)$$

Eq.(2) can be easily extended to the concept of conditional entropy with two variables. Given two discrete random variables I and J , conditional entropy is defined as

$$H(I|J) = - \sum_i \sum_j p(i,j) \log_2 p(i|j) \quad (3)$$

and it can be used to measure the information flow between two discrete random variables.

Consider two discrete random variables, I and J , with marginal probability distributions $p(i)$ and $p(j)$, and joint probability $p(i, j)$. Suppose they are stationary Markov processes of order k and l , respectively. For an order k Markov process I , Eq.(2) can be extended to

$$H^{(k)}(I) = - \sum_i p(i_t, i_{t-1}^{(k)}) \log p(i_t | i_{t-1}^{(k)}),$$

where $i_{t-1}^{(k)} = (i_{t-1}, \dots, i_{t-k})$. Analogously, the information flow from process J to I is measured by quantifying the deviation from the generalized Markov property $p(i_t | i_{t-1}^{(k)}) = p(i_t | i_{t-1}^{(k)}, j_{t-u}^{(l)})$ for an arbitrary source-target lag u , as follows:

$$T_{J \rightarrow I}^{(k,l)}(t, u) = \sum p(i_t, i_{t-1}^{(k)}, j_{t-u}^{(l)}) \log \frac{p(i_t | i_{t-1}^{(k)}, j_{t-u}^{(l)})}{p(i_t | i_{t-1}^{(k)})}. \quad (4)$$

Eq.(4) preserves the computational interpretation of TE as an information transfer, which is the only relevant option in keeping with Wiener's principle of causality [24]. The transfer entropy is known to be biased in small samples [14]. To correct any bias, [14] proposed the effective transfer entropy (ETE),

$$ETE_{J \rightarrow I}^{(k,l)}(t, u) = T_{J \rightarrow I}^{(k,l)}(t, u) - T_{J_{\text{shuffled}} \rightarrow I}^{(k,l)}(t, u). \quad (5)$$

where $T_{J_{\text{shuffled}} \rightarrow I}^{(k,l)}$ indicates the transfer entropy using a shuffled version of time series J . Shuffling randomly draws values from the original time series J and realigns them to generate a new time series. In this way, shuffling destroys the time series dependencies of J as well as the statistical dependencies between J and I . Note that $T_{J_{\text{shuffled}} \rightarrow I}^{(k,l)}$ converges to zero as the sample size increases, and any nonzero value of $T_{J_{\text{shuffled}} \rightarrow I}^{(k,l)}(t, u)$ is due to the small sample effects. To derive a consistent estimator, shuffling is repeated, and the average of the resulting shuffled transfer entropy estimates across all replications serves as an estimator for the small sample bias, which is subsequently subtracted from the Shannon or Rényi transfer entropy estimate to obtain a bias-corrected effective transfer entropy estimate.

Using Eq.(5), the time lag in a causal relationship $J \rightarrow I$ can be estimated by solving the optimization problem,

$$\hat{u} = \underset{u \in \mathbb{N}}{\operatorname{argmax}} ETE_{J \rightarrow I}^{(k,l)}(t, u). \quad (6)$$

In this study, we assume $k = \ell = 1$.

4 Methodology

We propose a new methodology for the time delay estimation of traffic congestion propagation based on lag-specific transfer entropy. Section 4.1 introduces times series decomposition and the bootstrap method. Sections 4.2 and 4.3 introduce normalization and symbolic encoding for calculating Transfer Entropy. Then, Section 4.4 defines the time delay estimator and discuss the hyperparameter tuning. Figure 2 illustrates the overview of the time delay estimation process.

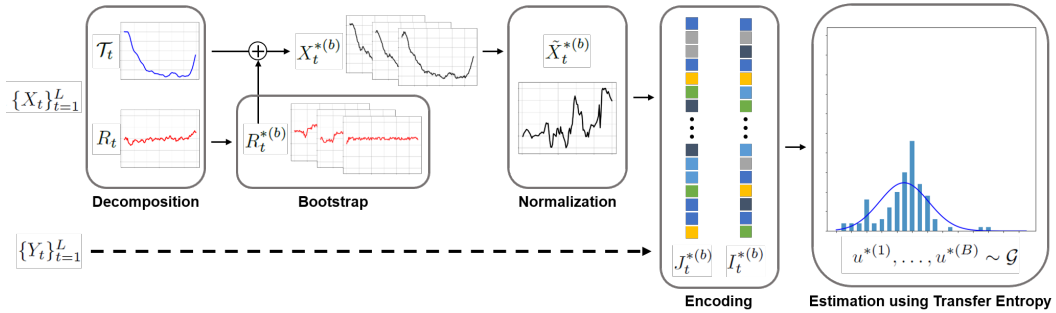


Figure 2: Overview of the time delay estimation process

4.1 Decomposition and Bootstrapping

Consider a time series of congested traffic speed data, $\{X_t\}_{t=1}^L$, which have properties of scale-dependence, nonlinearity, and non-stationarity. To identify the causal relationship effectively among such complicated time series, the application of appropriate preprocessing methods is essential.

First of all, we decompose a time series into a trend and its residual as follows:

$$\forall t, X_t = \mathcal{T}_t + R_t = \frac{1}{m} \sum_{j=0}^{m-1} X_{t-j} + R_t, \quad (7)$$

where \mathcal{T}_t is the trend component and R_t is the residual component. The trend component is a one-sided moving average of order m and the average of the forefront value at time t . The purpose of the trend component is to smooth a time series in order to estimate the underlying trend. After extracting the underlying trend from $\{X_t\}_{t=1}^L$, the residual time series $\{R_t\}_{t=1}^L$ is assumed to be a stationary Markov process. Based on $\{R_t\}_{t=1}^L$, we can generate the bootstrap residuals $\{R_t^{*(b)}\}_{t=1}^L$ as explained in Section 3.1. Once the bootstrap residuals are generated, then we easily obtain a bootstrap time series $\{X_t^{*(b)}\}_{t=1}^L$ by $\mathcal{T}_t + R_t^{*(b)}$ for $t = 1, \dots, L$.

4.2 Normalization

For the bootstrap time series, we apply nonlinear normalization with a sliding window for scale-dependent, nonlinear, and non-stationary time series of traffic speed data. To make them scale-independent and close to linear [23], a nonlinear function Φ , which is a standard normal CDF (cumulative distribution function), is applied. In addition, a sliding window technique has been applied to handle a non-stationary time series [16]. Let $\mathbf{X}_{t,w} = \left\{ X_k^{*(b)} \right\}_{k=t-w+1}^t$ be the forefront sequence of $X_t^{*(b)}$ with a sliding window size of w , and $F_{25,t}$, $F_{50,t}$, and $F_{75,t}$ be the 25th, 50th, and 75th percentiles of $\mathbf{X}_{t,w}$. Note that these percentiles depend on the location of the sliding window. We obtain a normalized time series as follows:

$$\left\{ \tilde{X}_t^{*(b)} \right\}_{t=1}^L, \quad (8)$$

where

$$\tilde{X}_t^{*(b)} = \Phi \left(0.5 \times \frac{X_t^{*(b)} - F_{50,t}}{F_{75,t} - F_{25,t}} \right). \quad (9)$$

To verify the effectiveness of the nonlinear method in Eq.(9), we compared its performances with existing normalization methods [16], including the min-max method $\left(\tilde{X}_t^{*(b)} = \frac{X_t^{*(b)}}{\max \mathbf{X}_{t,w}} \right)$, and a z-score method $\left(\tilde{X}_t^{*(b)} = \frac{X_t^{*(b)} - \mu(\mathbf{X}_{t,w})}{\sigma(\mathbf{X}_{t,w})} \right)$ with or without a sliding window technique in Section 5.

4.3 Symbolic Encoding and Transfer Entropy

To compute the lag-specific TE in Eq.(4), we discretize continuous data using symbolic encoding. This discretization can be obtained by partitioning the data into a finite number of bins. We denote the bounds specified for the n bins by q_1, q_2, \dots, q_{n-1} , where $q_1 < q_2 < \dots < q_{n-1}$. For the normalized time series in Eq.(8), we can obtain the encoded time series $\{J_t^{*(b)}\}_{t=1}^L$ by

$$J_t^{*(b)} = \begin{cases} 1 & \text{for } \tilde{X}_t^{*(b)} \leq q_1 \\ 2 & \text{for } q_1 < \tilde{X}_t^{*(b)} < q_2 \\ \vdots & \vdots \\ n & \text{for } \tilde{X}_t^{*(b)} \geq q_{n-1}. \end{cases} \quad (10)$$

The choice of bins is motivated by the distribution of the data. In the case in which tail observations are commonly of particular interest, binning is usually based on empirical quantiles such that the

left and right tail observations are selected into separate bins. For example, for $n = 3$, it is common to use the 5% and 95% empirical quantiles of the data as lower and upper bounds for binning, and thus the first (third) bin includes extremely low (high) data. In this study, we implemented symbolic encoding based on 5% and 95% empirical quantiles.

Consequently, we obtain $\{J_t^{*(b)}\}_{t=1}^L$ from $\{\tilde{X}_t^{*(b)}\}_{t=1}^L$ and $\{I_t^{*(b)}\}_{t=1}^L$ from $\{\tilde{Y}_t^{*(b)}\}_{t=1}^L$, respectively, for $b = 1, \dots, B$. Given $\{J_t^{*(b)}\}_{t=1}^L$ and $\{I_t^{*(b)}\}_{t=1}^L$, $b = 1, \dots, B$, we obtain a bootstrap sample of the time lag, $u^{*(1)}, \dots, u^{*(B)}$ using Eq.(6) as explained in Section 3.2.

4.4 Time Delay Estimation and Hyperparameter Tuning

Suppose that we obtain a bootstrap sample of the time lag, which follows a distribution \mathcal{G} ,

$$u^{*(1)}, \dots, u^{*(B)} \sim \mathcal{G}.$$

Note that we can obtain as many bootstrap observations as we want, but the distribution form of \mathcal{G} is unknown. In the process of congestion propagation between several connected roads, multiple bootstrap samples must be compared to follow their own distributions. To this end, we use two statistical functionals to quantify a distribution: the mean of a distribution (T_{mean}) and the variance of a distribution (T_{var}),

$$\mu = T_{\text{mean}}(\mathcal{G}), \quad \sigma^2 = T_{\text{var}}(\mathcal{G}). \quad (11)$$

Formally speaking, a statistical functional is a mapping $T : \mathcal{G} \rightarrow \mathbb{R}$, where \mathcal{G} is a collection of functions. However, we cannot compute μ and σ^2 in Eq.(11) because the distribution form of \mathcal{G} is unknown. Instead, we estimate μ and σ^2 by

$$\hat{\mu}_B = T_{\text{mean}}(\hat{\mathcal{G}}_B) = \frac{1}{B} \sum_{b=1}^B u^{*(b)} \quad \text{and} \quad \hat{\sigma}_B^2 = T_{\text{var}}(\hat{\mathcal{G}}_B) = \frac{1}{B} \sum_{b=1}^B (u^{*(b)})^2 - \hat{\mu}_B^2,$$

where $\hat{\mathcal{G}}_B$ is the empirical distribution function of $u^{*(b)}$, $b = 1, \dots, B$. As a result, we replace Eq.(6) by the bootstrap estimate $\hat{\mu}_B$ for the time delay estimation.

Proposition 1. *Let $u^{*(1)}, \dots, u^{*(B)}$ be a bootstrap sample and $E(u^{*(b)}) = \mu$, $\text{Var}(u^{*(b)}) = \sigma^2$. Then, sample mean $\hat{\mu}_B = \frac{1}{B} \sum_{b=1}^B u^{*(b)}$ approximately follows $\mathcal{N}(\mu, \frac{1}{B} \hat{\sigma}_B^2)$, where $\hat{\sigma}_B^2$ is the sample variance of the bootstrap sample.*

Proof. Since $\hat{\sigma}_B^2 \rightarrow \sigma^2$ in probability,

$$\frac{\sqrt{B}(\hat{\mu}_B - \mu)}{\hat{\sigma}_B} = \frac{\sigma}{\hat{\sigma}_B} \frac{\sqrt{B}(\hat{\mu}_B - \mu)}{\sigma} \xrightarrow{d} \mathcal{N}(0, 1)$$

by the Central Limit Theorem and Slutsky's Theorem [4]. Hence, $\hat{\mu}_B$ approximately follows a normal distribution,

$$\hat{\mu}_B \sim \mathcal{N}\left(\mu, \frac{1}{B} \hat{\sigma}_B^2\right).$$

□

Proposition 1 presents that $\frac{1}{B} \hat{\sigma}_B^2$ quantifies the uncertainty of the bootstrap estimate $\hat{\mu}_B$. Therefore, $\hat{\sigma}_B^2$ can be used as an indicator of whether there exists a causal relationship. The larger the value of $\hat{\sigma}_B^2$, the less likely a causality exists.

Two hyperparameters are involved in the time delay estimation: the length of time series (L) and the sliding window size (w). Depending on the hyperparameter values, we obtain different bootstrap samples and accordingly different bootstrap estimates. Consequently, it is crucial to choose a set of optimal hyperparameters for reliable time delay estimation. For hyperparameter tuning in the time delay estimation, we used a grid search to find a set of hyperparameters that minimize $\frac{1}{B} \hat{\sigma}_B^2$, because true μ is unknown in reality.

5 Simulation Studies

The proposed method was validated using the simulated data. Two time series, $\{X_t\}_{t=1}^{120}$ and $\{Y_t\}_{t=1}^{120}$, are generated by

$$X_t = \begin{cases} 100 + \epsilon_{x,t} & \text{for } t < 10 \\ 0.95X_{t-1} + \epsilon_{x,t} & \text{for } 10 \leq t < 95, \\ 1.10X_{t-1} + \epsilon_{x,t} & \text{for } t \geq 120 \end{cases} \quad Y_t = \begin{cases} 70 + \epsilon_{y,t} & \text{for } t < 10 \\ 0.5X_{t-u_0} + 20 + \epsilon_{y,t} & \text{for } t \geq 10 \end{cases}$$

where $\epsilon_{x,t} \sim \mathcal{N}(0, 1)$ and $\epsilon_{y,t} \sim \mathcal{N}(0, 1)$, and a predetermined source-target lag (u_0) exists such that a significant information flow from X to Y is formed, but not vice versa. Figure 3(a) depicts two time series with $u_0 = 10$. The black solid line and red dotted line represent $\{X_t\}_{t=1}^{120}$ and $\{Y_t\}_{t=1}^{120}$, respectively. These simulated data represent the case of congestion on a road, i.e., road R_X , which propagates to an upcoming road, i.e., road R_Y . We can assume that there was a traffic accident on road R_X at $t = 10$ and that the congestion was resolved at $t = 95$. With $u_0 = 10$, the congestion on R_X propagates to road R_Y .

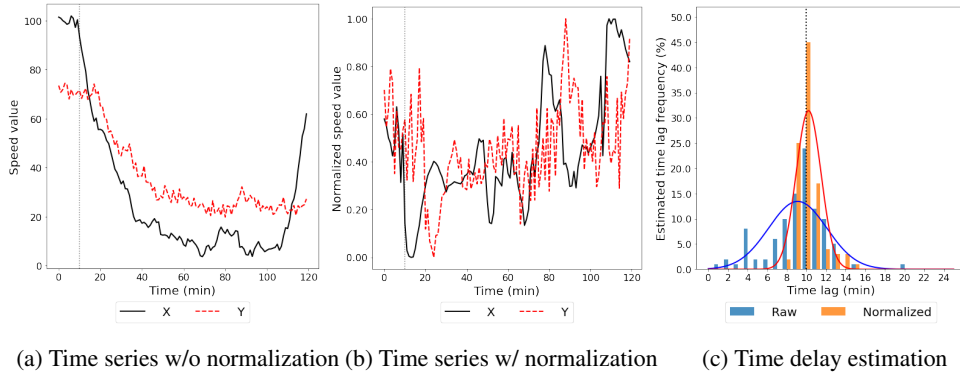


Figure 3: Speed values and bootstrap results

We decomposed the normalized time series using Eq.(7) with $m = 2$. Then, the Markov bootstrap was used to generate bootstrap samples, as explained in Section 4.1. Figure 3(b) shows the results of nonlinear normalization with a sliding window ($w = 20$). Figure 3(c) compares the distributions of bootstrap samples obtained based on two time series without normalization in Figure 3(a) and two time series with normalization in Figure 3(b). Based on bootstrap samples, we obtained two statistical functionals $(\hat{\mu}_B, \hat{\sigma}_B^2)$ for both cases. The red and blue lines in Figure 3(c) depict $\mathcal{N}(8.94, 3.04^2)$ and $\mathcal{N}(10.26, 1.26^2)$, respectively. As a result, we confirmed that normalization with a sliding window improved the accuracy of the time delay estimation.

An additional simulation was carried out to compare the performance of the time delay estimation for various normalization methods as well as different lengths of sliding windows ($w = 10, 20, 30, 40, 120$). The performance under different settings was evaluated by $\hat{\mu}_B$, $\hat{\sigma}_B^2$, and MAE, where $MAE = \frac{1}{B} \sum_{i=1}^B |\hat{\mu}_i - u_0|$. The closer the value is to u_0 , the better the estimate $\hat{\mu}_B$. The smaller the values of $\hat{\sigma}_B^2$ and MAE are, the better the results.

The detailed results are summarized in Table 1. This results confirm that nonlinear normalization generally performs better than existing methods, including the min-max method and the z-score method, and the hyperparameter w can be determined by the one that minimizes $\hat{\sigma}_B^2$ as suggested in Section 4.4. We implemented the effective transfer entropy in R within the `RTransferEntropy` package (version 0.2.13) [3].

6 Real Data Example : An Incident-driven Traffic Congestion Propagation

The proposed method was applied to discover causal relationships between roads near two real traffic accident cases that occurred in the city of Seoul. The star in Figure 4 represents the exact location where the accident occurred. Figure 4 illustrates two road networks related to the accidents: case 1 represents a simple road network having a small number of propagation paths involved, whereas

Table 1: Simulations results comparison ($u_0 = 10$)

Methods	Metrics	Window length				
		10	20	30	40	120 (all)
min-max	$\hat{\mu}_B$	13.15	10.71	8.58	10.05	9.17
	$\hat{\sigma}_B^2$	22.81	10.89	5.78	11.65	12.52
	MAE	4.51	2.17	1.90	2.31	2.43
z-score	$\hat{\mu}_B$	9.88	10.07	10.21	12.05	9.07
	$\hat{\sigma}_B^2$	9.85	12.19	18.51	19.33	10.11
	MAE	1.64	2.15	2.79	3.35	2.29
nonlinear	$\hat{\mu}_B$	10.31	10.22	10.52	10.76	9.30
	$\hat{\sigma}_B^2$	8.19	1.59	1.97	2.52	13.41
	MAE	1.33	0.78	1.16	1.46	2.44

case 2 shows a complex road network having many propagation paths involved. Here, we define the propagation path by a sequence of incoming roads in the opposite direction of the traffic flow. For example, case 1 has one propagation path, $[A, B, C, D]$, whereas case 2 has five propagation paths, $[A, B, C, D]$, $[A, E, F, G]$, $[A, H, I, J]$, $[A, H, K, M]$ and $[A, H, K, L]$. Traffic congestion caused by traffic accidents propagates along the propagation paths. The k th element in the propagation path is denoted as Hop($k-1$). In this study, we investigated up to $k = 4$. The black, red, blue, and green line segments in the figure indicate Hop0, Hop1, Hop2, and Hop3, respectively. Experiments code is developed by python 3.8 on AMD Ryzen Threadripper 3970X workstation.

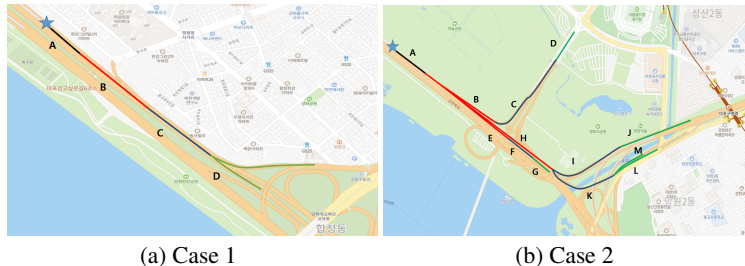


Figure 4: Simple and complex road networks where congestion occurred from incidents

6.1 Case 1: Simple Traffic Network

The car accident occurred on September 8, 2020, at 06:44 AM. TE was calculated using average speed data recorded at one-minute intervals from the previous 1 hour to the next 2 hours based on the time when the incident was reported. We investigate one of the main propagation paths $[A, B, C, D]$ and its causal impact from A to the nearby roads, which has a direct impact. In Figure 5, the original time series without normalization estimates the time lag inconsistently. By contrast, the time series with nonlinear normalization provides a consistent estimation of the time lag, which is increased by each hop. Furthermore, Table 2 concludes that nonlinear normalization presents a smaller $\hat{\sigma}_B^2$, which proves the higher accuracy of $\hat{\mu}_B$.

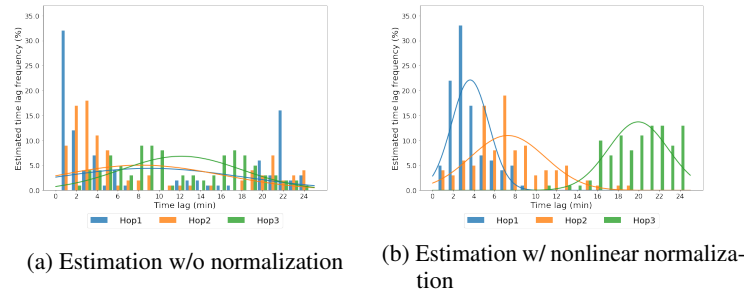


Figure 5: Time delay estimation for Case 1

Table 2: Time delay estimation comparison for Case 1

Normalization	Path	Hop1		Hop2		Hop3	
		$\hat{\mu}_B$	$\hat{\sigma}_B^2$	$\hat{\mu}_B$	$\hat{\sigma}_B^2$	$\hat{\mu}_B$	$\hat{\sigma}_B^2$
w/o normalization	$[A, B, C, D]$	9.62	83.70	8.07	61.31	12.08	34.83
nonlinear	$[A, B, C, D]$	3.60	2.88	7.30	13.83	19.97	8.93

6.2 Case 2: Complex Traffic Network

The accident occurred on September 4, 2020, at 22:16 PM and affected total five paths. For each path, the previous 1 hour and following 2 hours are considered for time delay estimation. Here, we only considered nonlinear normalization and the hyperparameters were tuned by using a grid search.

Figure 6 illustrates some of the time delay estimation results. In path 1 ($[A, B, C, D]$), the estimated distribution seems uniform for all available time lags, which means there is no specific causal relationship. As Table 3 shows the values of corresponding $\hat{\sigma}_B^2$ are larger than others. Paths 4 and 5 seem to be congested by the root road propagating to the 3-hop range. In the case of path 5 ($[A, H, K, L]$), the mean of the estimated time lag $\hat{\mu}_B$ monotonically increases with the hops. This can be evidence of a sequential causal relationship along this path, and congestion from an accident road will propagate along this path.

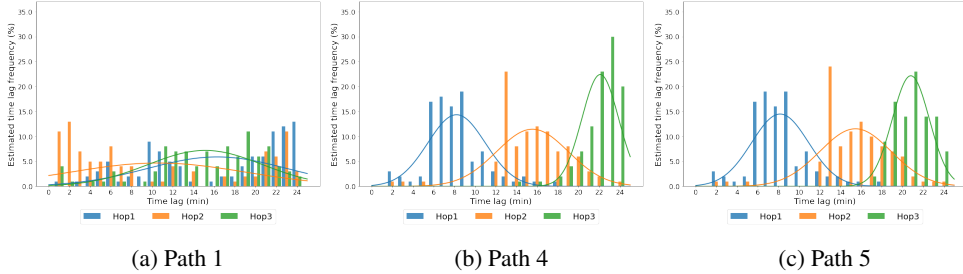


Figure 6: Time delay estimation for Case 2

Table 3: Time delay estimation using nonlinear normalization for Case 2

Path	Hop1		Hop2		Hop3	
	$\hat{\mu}_B$	$\hat{\sigma}_B^2$	$\hat{\mu}_B$	$\hat{\sigma}_B^2$	$\hat{\mu}_B$	$\hat{\sigma}_B^2$
$[A, B, C, D]$	16.03	47.09	11.59	73.56	15.17	30.46
$[A, E, F, G]$	4.93	19.19	7.20	21.58	7.04	14.54
$[A, H, I, J]$	8.21	7.97	12.13	7.03	15.72	57.16
$[A, H, K, M]$	8.23	7.62	15.65	9.01	22.06	3.24
$[A, H, K, L]$	8.22	7.67	15.55	11.01	20.75	3.17

7 Conclusion

We presented a novel method for estimating the time delay of inflow roads in congestion situations in a traffic network. Traffic congestion propagates along with its inflow roads, and the root road has a causal relationship with its inflow roads. We applied a lag-specific TE estimator to traffic speed data of a network normalized by our proposed method, which includes the concept of nonlinear normalization with the sliding window technique. The proposed nonlinear normalization showed better results when comparing the estimated time lag in the non-stationary time series than other cases where other normalization techniques have been adopted. Furthermore, the bootstrap technique and its density estimation of statistical functionals enable a quantitative estimation of the time delay.

However, there are limitations that need to be addressed. TE is sensitive to hyperparameters. Therefore, it is important to find optimal hyperparameters for reliable delay estimation. In this paper, we proposed a grid search based on $\hat{\sigma}_B^2$, but future research is needed for further improvement.

References

- [1] Lionel Barnett, Adam B Barrett, and Anil K Seth. Granger causality and transfer entropy are equivalent for gaussian variables. *Physical review letters*, 103(23):238701, 2009.
- [2] Sanchita Basak, Abhishek Dubey, and Leao Bruno. Analyzing the cascading effect of traffic congestion using lstm networks. In *2019 IEEE International Conference on Big Data (Big Data)*, pages 2144–2153. IEEE, 2019.
- [3] Simon Behrendt, Thomas Dimpfl, Franziska J Peter, and David J Zimmermann. Rtransferentropy—quantifying information flow between different time series using effective transfer entropy. *SoftwareX*, 10:100265, 2019.
- [4] George Casella and Roger L Berger. *Statistical inference*. Cengage Learning, 2021.
- [5] Xiaolei Di, Yu Xiao, Chao Zhu, Yang Deng, Qinpei Zhao, and Weixiong Rao. Traffic congestion prediction by spatiotemporal propagation patterns. In *2019 20th IEEE International Conference on Mobile Data Management (MDM)*, pages 298–303. IEEE, 2019.
- [6] Luca Faes, Daniele Marinazzo, Alessandro Montalto, and Giandomenico Nollo. Lag-specific transfer entropy as a tool to assess cardiovascular and cardiorespiratory information transfer. *IEEE Transactions on Biomedical Engineering*, 61(10):2556–2568, 2014.
- [7] Clive WJ Granger. Investigating causal relations by econometric models and cross-spectral methods. *Econometrica: journal of the Econometric Society*, pages 424–438, 1969.
- [8] Jens-Peter Kreiss and Soumendra Nath Lahiri. Bootstrap methods for time series. In *Handbook of statistics*, volume 30, pages 3–26. Elsevier, 2012.
- [9] Hodong Lee, Changsoo Kim, Sanha Lim, and Jong Min Lee. Data-driven fault diagnosis for chemical processes using transfer entropy and graphical lasso. *Computers & Chemical Engineering*, 142:107064, 2020.
- [10] Joon Lee, Shamim Nemati, Ikaro Silva, Bradley A Edwards, James P Butler, and Atul Malhotra. Transfer entropy estimation and directional coupling change detection in biomedical time series. *Biomedical engineering online*, 11(1):1–17, 2012.
- [11] Wei-Hsun Lee, Shian-Shyong Tseng, Jin-Lih Shieh, and Hsiao-Han Chen. Discovering traffic bottlenecks in an urban network by spatiotemporal data mining on location-based services. *IEEE Transactions on Intelligent Transportation Systems*, 12(4):1047–1056, 2011.
- [12] Wei Liu, Yu Zheng, Sanjay Chawla, Jing Yuan, and Xie Xing. Discovering spatio-temporal causal interactions in traffic data streams. In *Proceedings of the 17th ACM SIGKDD international conference on Knowledge discovery and data mining*, pages 1010–1018, 2011.
- [13] Yi Luo, Bhushan Gopaluni, Yuan Xu, Liang Cao, and Qun-Xiong Zhu. A novel approach to alarm causality analysis using active dynamic transfer entropy. *Industrial & Engineering Chemistry Research*, 59(18):8661–8673, 2020.
- [14] Robert Marschinski and Holger Kantz. Analysing the information flow between financial time series. *The European Physical Journal B-Condensed Matter and Complex Systems*, 30(2):275–281, 2002.
- [15] Hoang Nguyen, Wei Liu, and Fang Chen. Discovering congestion propagation patterns in spatio-temporal traffic data. *IEEE Transactions on Big Data*, 3(2):169–180, 2016.
- [16] Eduardo Ogasawara, Leonardo C Martinez, Daniel De Oliveira, Geraldo Zimbrão, Gisele L Pappa, and Marta Mattoso. Adaptive normalization: A novel data normalization approach for non-stationary time series. In *The 2010 International Joint Conference on Neural Networks (IJCNN)*, pages 1–8. IEEE, 2010.
- [17] Alberto Porta, S Guzzetti, N Montano, M Pagani, Virend Somers, A Malliani, Giuseppe Baselli, and Sergio Cerutti. Information domain analysis of cardiovascular variability signals: evaluation of regularity, synchronisation and co-ordination. *Medical and Biological Engineering and Computing*, 38(2):180–188, 2000.
- [18] Thomas Schreiber. Measuring information transfer. *Physical review letters*, 85(2):461, 2000.
- [19] Ahmet Sensoy, Cihat Sobaci, Sadri Sensoy, and Fatih Alali. Effective transfer entropy approach to information flow between exchange rates and stock markets. *Chaos, solitons & fractals*, 68:180–185, 2014.
- [20] Claude E Shannon. A mathematical theory of communication. *The Bell system technical journal*, 27(3):379–423, 1948.
- [21] Yue Teng and Pengjian Shang. Transfer entropy coefficient: Quantifying level of information flow between financial time series. *Physica A: Statistical Mechanics and its Applications*, 469:60–70, 2017.
- [22] Raul Vicente, Michael Wibral, Michael Lindner, and Gordon Pipa. Transfer entropy—a model-free measure of effective connectivity for the neurosciences. *Journal of computational neuroscience*, 30(1):45–67, 2011.

- [23] Jingyu Wang, Sheng Su, Yinhong Li, Jinfu Chen, and Dongyuan Shi. Desaturated probability integral transform for normalizing power system measurements in data-driven manipulation detection. In *2019 IEEE Power & Energy Society General Meeting (PESGM)*, pages 1–5. IEEE, 2019.
- [24] Michael Wibral, Nicolae Pampu, Viola Priesemann, Felix Siebenhühner, Hannes Seiwert, Michael Lindner, Joseph T Lizier, and Raul Vicente. Measuring information-transfer delays. *PloS one*, 8(2):e55809, 2013.
- [25] Yinhong Xiao, Yaoshuai Zhao, Ge Wu, and Yizhen Jing. Study on delay propagation relations among airports based on transfer entropy. *IEEE Access*, 8:97103–97113, 2020.
- [26] Haoyi Xiong, Amin Vahedian, Xun Zhou, Yanhua Li, and Jun Luo. Predicting traffic congestion propagation patterns: a propagation graph approach. In *Proceedings of the 11th ACM SIGSPATIAL International Workshop on Computational Transportation Science*, pages 60–69, 2018.
- [27] Can-Zhong Yao and Hong-Yu Li. Effective transfer entropy approach to information flow among epu, investor sentiment and stock market. *Front. Phys.* 8: 206. doi: 10.3389/fphy, 2020.
- [28] Sen Zhang, Yong Yao, Jie Hu, Yong Zhao, Shaobo Li, and Jianjun Hu. Deep autoencoder neural networks for short-term traffic congestion prediction of transportation networks. *Sensors*, 19(10):2229, 2019.

A Detailed results of simulation studies

A.1 Selected sample

We applied three different normalization with or without sliding window. Figure 8 shows the normalization results for the time series X and Y respectively. (a), (b) and (c) are each normalization methods without sliding window and (d), (e) and (f) are normalization methods with sliding window ($w=20$). Suggested non-linear normalization with sliding window approach can reflect the local volatility compare to other methods.

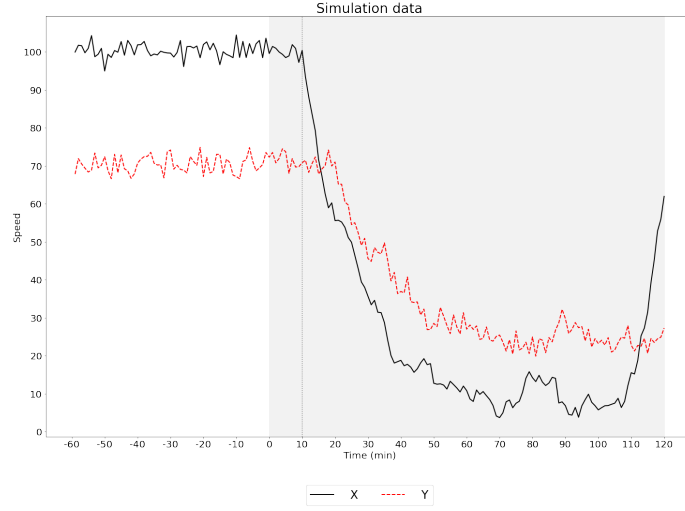


Figure 7: Simulation data of X and Y

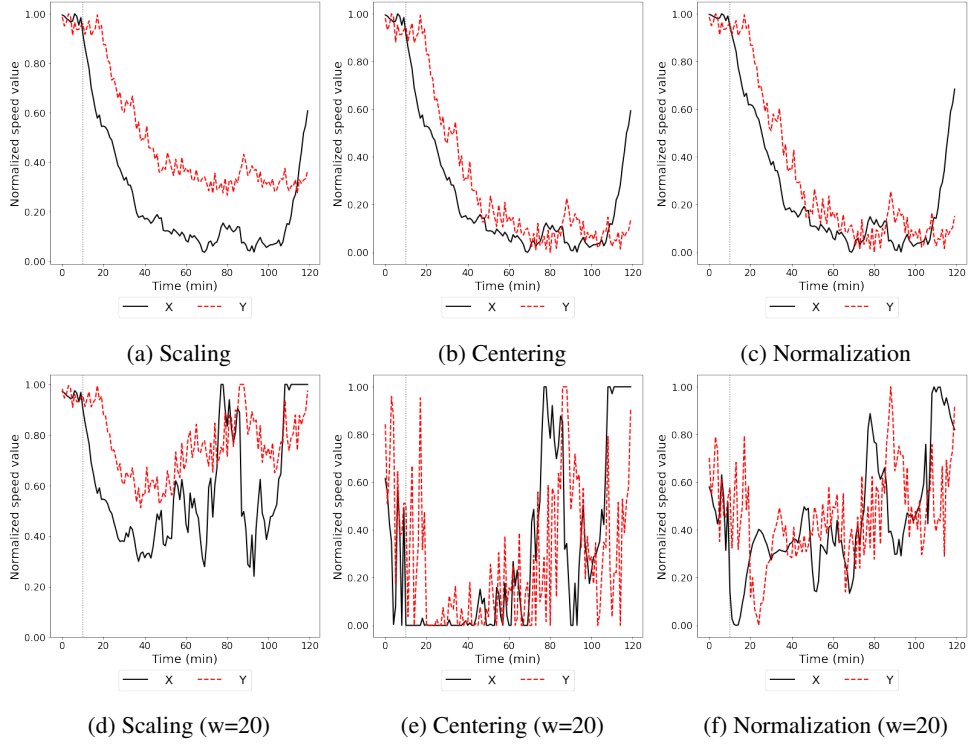


Figure 8: Comparison of normalization methods to speed values

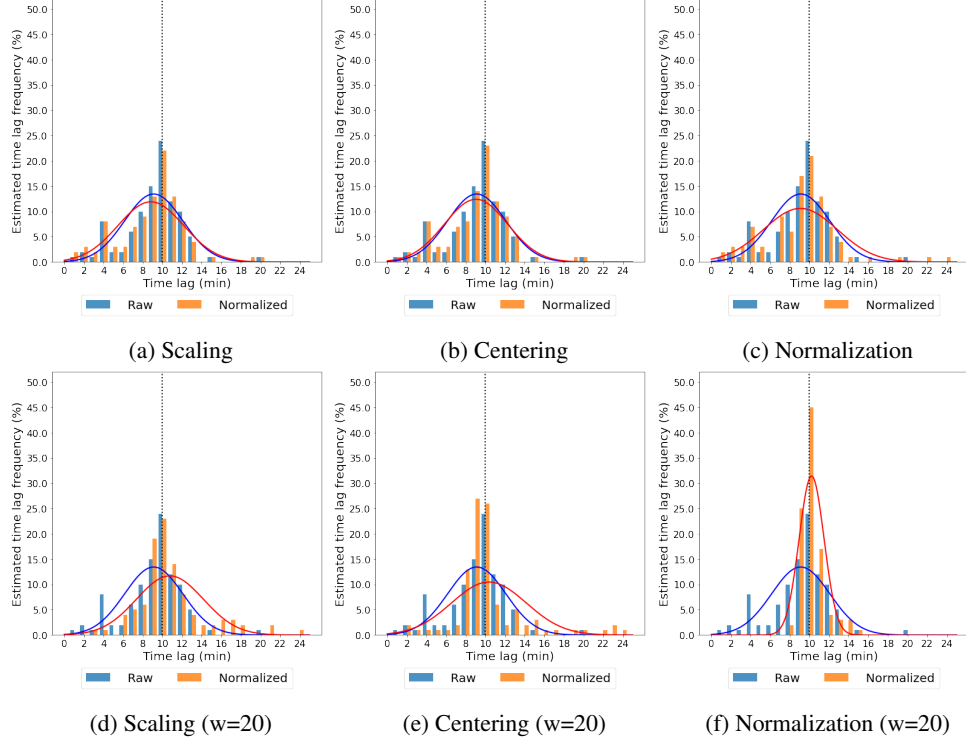


Figure 9: Comparison of Bootstrap results

Furthermore, Figure 9 shows comparison of time delay estimation from bootstrap samples. Suggested non-linear normalization and sliding window approach outperform to find the estimated time lag. Also, it shows small MAE value, comparing with the true time lag. In the real case, we cannot compare estimated time lag and true value. However suggested approach can estimate time lag with small standard deviation compare to other methods.

Experiments code is developed by python 3.8 on AMD Ryzen Threadripper 3970X 32-Core processor workstation. We implemented the effective transfer entropy in R within the *RTransferEntropy* package (version 0.2.13) [3]. Proposed code utilize multiprocessing to bootstrap efficiently. Simulation code is uploaded on <https://github.com/yongkyung-oh/TE-propagation>.

A.2 Random samples test

To verify the scalability and robustness, we tested with 100 different time series pair X and Y . Three different time lag (5,10,15) and different level of noise (1,2,3) are considered. For example, noise 2 means $\epsilon_{x,t} \sim \mathcal{N}(0, 2)$ and $\epsilon_{y,t} \sim \mathcal{N}(0, 2)$. We use $B = 100$ for each case and average the $\hat{\sigma}_B$ and MAE. Table 5 and Table 4 show the results of 100 simulations. Second column of the table indicates the size of sliding window. The value in the table shows average and standard deviation of the scores though 100 simulations.

Similar with one simulation case, normalization show the best performance in the perspective of $\hat{\sigma}_B$ and MAE. Here we interpret smaller $\hat{\sigma}_B$ and MAE means much confident estimation of true time lag. In case of MAE, scaling works better in some case, when window size is fitted well. However, it is hard to find the optimal sliding window size in the real situation. Compare to that, normalization approach shows better despite of window size. In other words, if we use sliding window normalization with unknown optimal window size, normalization is the best option in the perspective of $\hat{\sigma}_B$ MAE. Therefore, normalization with sliding window is implemented for the real incident cases.

Table 4: 100 simulations results comparison: $\hat{\sigma}_B$

Methods	Lag	5			10			15		
		Noise	1	2	3	1	2	3	1	2
w/o normalization		5.04 (0.35)	7.75 (0.69)	4.58 (0.30)	3.49 (0.11)	4.36 (0.17)	4.93 (0.09)	4.30 (0.39)	4.03 (0.03)	4.29 (0.12)
min-max	20	8.27 (0.43)	4.49 (1.11)	4.38 (1.13)	3.76 (0.33)	3.32 (0.40)	3.29 (0.49)	4.89 (0.21)	3.30 (0.41)	3.33 (0.44)
	30	2.75 (0.72)	3.86 (0.41)	3.76 (0.34)	4.29 (0.13)	5.20 (0.40)	5.09 (0.31)	6.80 (0.76)	8.28 (1.12)	6.05 (0.46)
	40	2.60 (0.66)	3.19 (0.33)	3.82 (0.33)	3.60 (0.23)	3.72 (0.31)	3.40 (0.11)	3.71 (0.76)	3.62 (0.25)	3.57 (0.12)
	all	5.03 (0.34)	7.77 (0.69)	4.58 (0.30)	3.51 (0.10)	4.35 (0.17)	4.92 (0.09)	4.29 (0.39)	4.03 (0.03)	4.30 (0.12)
	(120)									
z-score	20	5.33 (1.08)	6.24 (1.19)	5.38 (1.19)	5.44 (0.95)	4.72 (0.31)	5.14 (0.21)	6.42 (0.04)	4.69 (0.10)	4.77 (0.11)
	30	4.80 (0.90)	5.26 (0.68)	5.75 (0.64)	4.21 (0.53)	4.23 (0.60)	4.88 (0.30)	7.27 (0.55)	4.97 (0.49)	5.06 (0.52)
	40	4.08 (0.76)	6.81 (0.35)	8.04 (0.24)	4.23 (0.31)	3.82 (0.71)	4.60 (0.56)	7.52 (0.75)	6.10 (0.44)	5.90 (0.10)
	all	5.02 (0.34)	7.77 (0.68)	4.57 (0.31)	3.50 (0.10)	4.35 (0.17)	4.93 (0.10)	4.30 (0.39)	4.02 (0.03)	4.30 (0.12)
	(120)									
non-linear	20	3.37 (0.11)	3.69 (0.88)	4.26 (0.93)	2.03 (0.39)	1.97 (0.03)	3.24 (0.43)	2.07 (0.06)	1.78 (0.10)	3.41 (0.49)
	30	2.58 (0.08)	2.49 (0.58)	2.69 (0.46)	2.94 (0.09)	1.70 (0.61)	2.46 (0.11)	2.39 (0.10)	1.72 (0.20)	1.98 (0.31)
	40	2.72 (0.38)	3.07 (1.21)	2.68 (0.76)	3.87 (0.10)	2.70 (0.83)	2.98 (0.64)	2.68 (0.15)	2.37 (0.27)	2.93 (0.30)
	all	3.59 (0.12)	7.60 (0.62)	4.53 (0.32)	3.31 (0.17)	4.04 (0.04)	4.75 (0.17)	3.94 (0.24)	3.92 (0.06)	4.32 (0.10)
	(120)									

Table 5: 100 simulations results comparison: MAE

Methods	Lag	5			10			15		
		Noise	1	2	3	1	2	3	1	2
w/o normalization		1.45 (0.33)	3.38 (0.46)	1.50 (0.32)	0.49 (0.10)	0.24 (0.10)	1.06 (0.30)	1.73 (0.18)	0.78 (0.13)	0.19 (0.12)
min-max	20	4.17 (0.69)	1.03 (0.96)	1.27 (1.00)	0.08 (0.10)	1.17 (0.03)	1.15 (0.08)	2.07 (0.17)	1.25 (0.14)	0.85 (0.03)
	30	0.46 (0.82)	2.03 (0.40)	1.66 (0.38)	1.27 (0.14)	3.45 (0.53)	2.55 (0.32)	5.13 (0.98)	6.98 (1.30)	3.71 (0.57)
	40	1.41 (0.53)	0.66 (0.10)	1.77 (0.30)	1.61 (0.03)	2.25 (0.51)	1.57 (0.34)	2.40 (0.08)	2.49 (0.41)	2.00 (0.45)
	all	1.44 (0.33)	3.39 (0.45)	1.51 (0.32)	0.49 (0.10)	0.25 (0.09)	1.07 (0.31)	1.74 (0.18)	0.77 (0.12)	0.19 (0.12)
	(120)									
z-score	20	3.36 (0.99)	4.01 (1.10)	3.23 (0.97)	1.68 (0.97)	2.41 (0.30)	2.99 (0.35)	2.24 (0.10)	1.88 (0.34)	2.36 (0.30)
	30	1.91 (1.19)	3.87 (0.42)	3.95 (0.39)	1.02 (0.15)	0.97 (0.40)	1.32 (0.12)	4.83 (1.07)	0.72 (0.45)	0.34 (0.57)
	40	1.52 (1.00)	5.07 (0.11)	6.31 (0.15)	1.22 (0.08)	0.45 (0.74)	1.68 (0.47)	6.17 (1.36)	2.60 (0.36)	1.45 (0.30)
	all	1.44 (0.33)	3.40 (0.44)	1.50 (0.32)	0.50 (0.10)	0.25 (0.10)	1.06 (0.31)	1.74 (0.19)	0.78 (0.13)	0.20 (0.13)
	(120)									
non-linear	20	1.04 (0.08)	2.73 (0.28)	3.34 (0.43)	0.64 (0.20)	0.12 (0.13)	1.43 (0.12)	0.28 (0.05)	0.11 (0.03)	1.83 (0.07)
	30	0.81 (0.02)	1.45 (0.05)	1.99 (0.07)	0.33 (0.06)	0.57 (0.20)	0.77 (0.15)	0.23 (0.03)	0.10 (0.08)	0.74 (0.13)
	40	0.55 (0.29)	1.65 (0.71)	1.23 (0.44)	0.35 (0.09)	0.32 (0.66)	1.51 (0.43)	0.38 (0.04)	0.36 (0.24)	1.79 (0.04)
	all	0.78 (0.12)	3.11 (0.30)	1.54 (0.40)	0.38 (0.08)	0.42 (0.10)	0.91 (0.32)	1.27 (0.09)	0.65 (0.15)	0.17 (0.19)
	(120)									

B Detailed results of real data example

B.1 Case 1: Simplex traffic network

Accident occurred at the 4th lane out of 4 lanes of the expressway on September 8th 06:44. Previous 1 hour and following 2 hours are considered to calculate transfer entropy. We investigate the one of the main propagation path $[A, B, C, D]$ and its causal impact from A to near roads, which has direct impact. Figure 11 and Figure 12 shows the ETE value of one sample and estimated time lag distribution by bootstrap.



Figure 10: Case 1. Simple traffic network

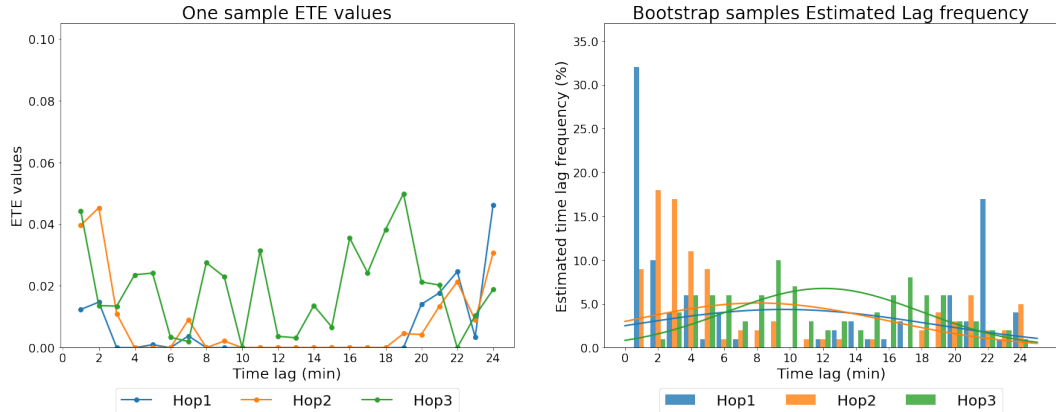


Figure 11: Case 1. ETE value and estimated time lag by hop

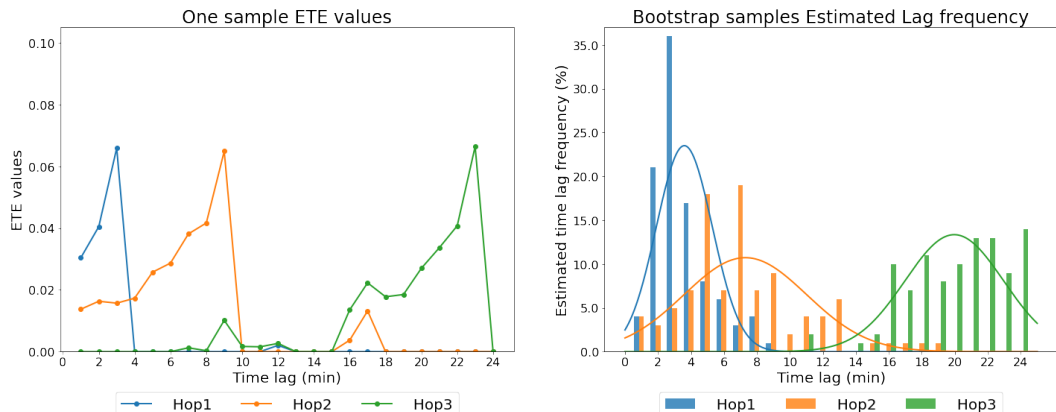


Figure 12: Case 1. ETE value and estimated time lag by hop

B.2 Case 2: Complex traffic network

Accident occurred at the 2nd lane out of 5 lanes of the expressway on September 4th 22:16. Previous 1 hour and following 2 hours are considered to calculate transfer entropy. Case 2 has five propagation paths, $[A, B, C, D]$, $[A, E, F, G]$, $[A, H, I, J]$, $[A, H, K, M]$ and $[A, H, K, L]$. Some paths are directly affected by root road and other are not affected. Suggested approach can investigate which road has causal relationship with accident road. Furthermore, it provide estimated time lag of congestion propagation using transfer entropy.



Figure 13: Case 2. Complex traffic network

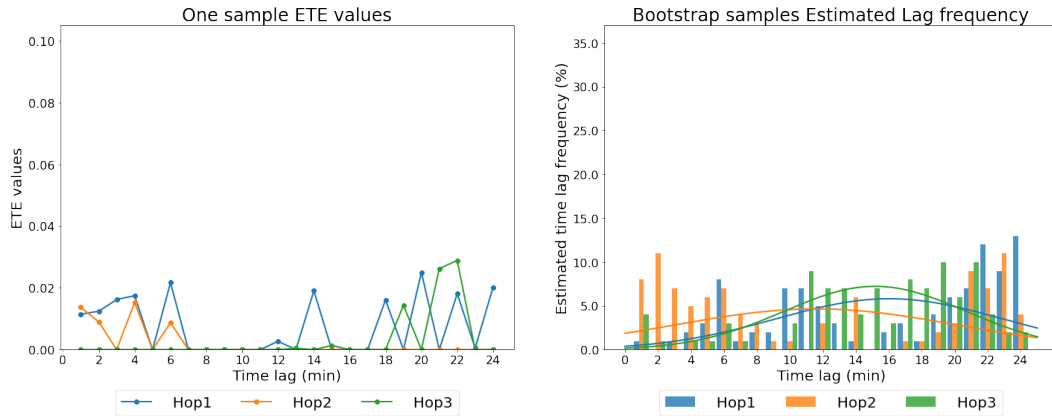


Figure 14: Case 2-1. ETE value and estimated time lag by hop

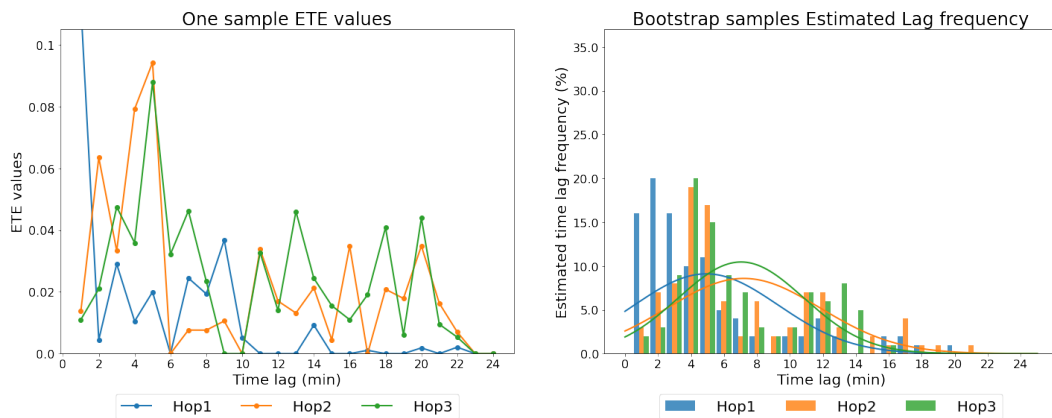


Figure 15: Case 2-2. ETE value and estimated time lag by hop

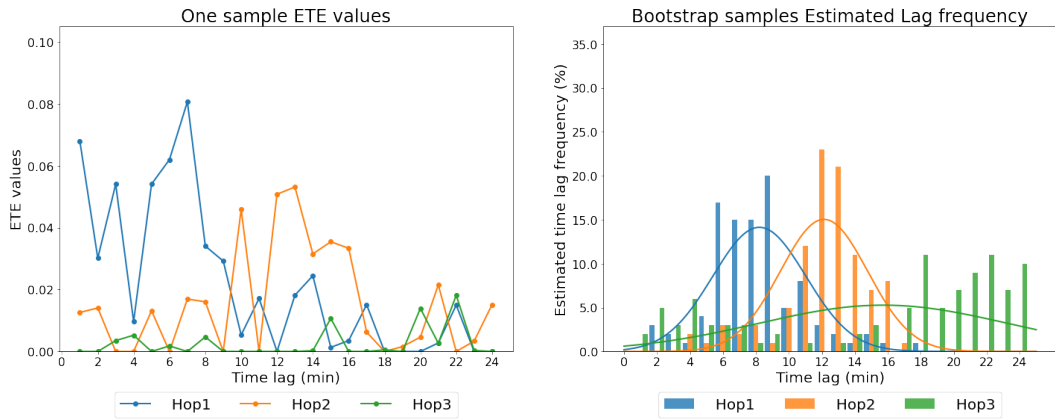


Figure 16: Case 2-3. ETE value and estimated time lag by hop

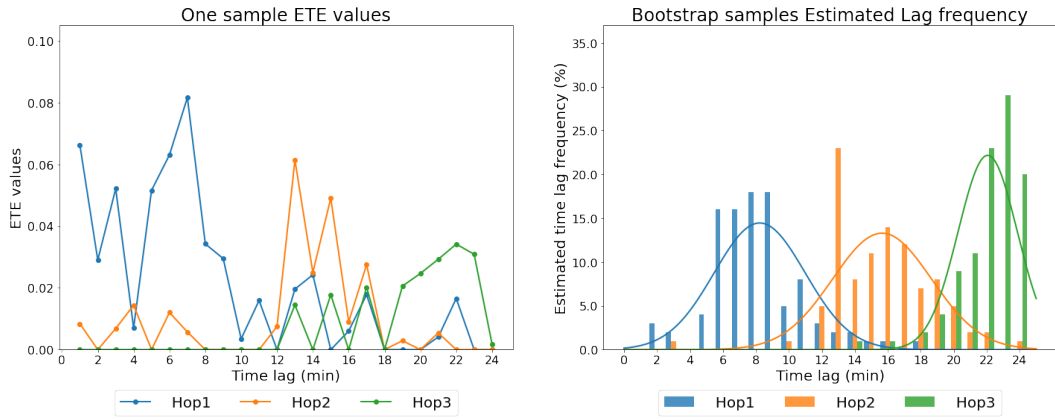


Figure 17: Case 2-4. ETE value and estimated time lag by hop

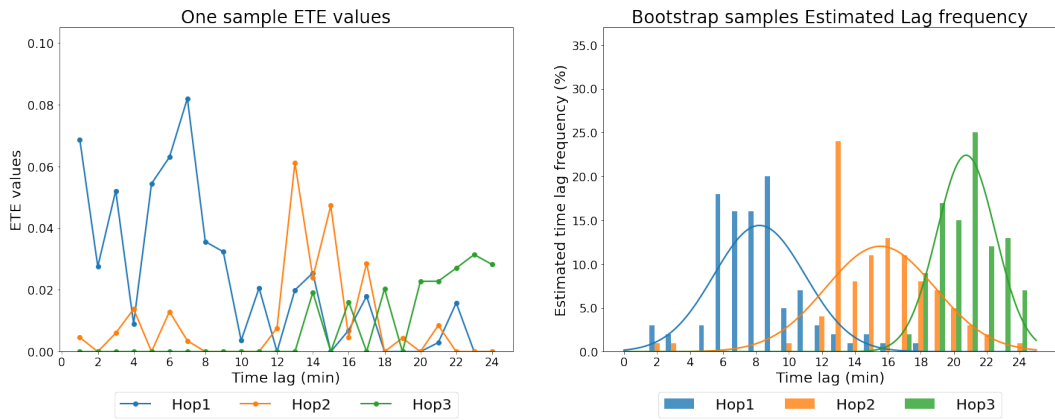


Figure 18: Case 2-5. ETE value and estimated time lag by hop